Supporting Information

One-step Synthesis of Na-Sn Alloy with Internal 3-D $Na_{15}Sn_4$ Support for Fast and Stable Na Metal Batteries

Olusola John Dahunsi, Bomin Li, Siyuan Gao, Ke Lu, Fan Xia, Tao Xu, Yingwen Cheng *

Department of Chemistry and Biochemistry, Northern Illinois University, DeKalb, IL 60115 United States

*E-mail: ycheng@niu.edu

1. Complete experimental details, materials, and methods

Materials: diglyme (>99.0%, TCI), $NaPF_6$ (98.5%, Alfa Aesar), sodium sticks (99%, Alfa Aesar), tin foil (99.8%, Alfa Aesar), oxalic acid (Fischer Scientific), carbon nanotubes (>95 wt.%, Cheap tubes Inc), NaH_2PO_4 $2H_2O$ (99%, Alfa Aesar), isopropanol (99%, Fischer Scientific), PTFE dispersion (Polysciences Inc.), molecular sieve 4A (Alfa Aesar), super-P carbon black (MTI Corp.). All chemicals were used as received without further purification.

Materials synthesis

Synthesis of NaSn alloy was performed in an Ar filled MBraun Labstar glovebox where H_2O and O_2 concentrations were both < 0.5 ppm. In a typical procedure, 0.26 g tin foil was immersed in 2.76 g molten Na metal in a crucible at 400°C. The molten mixture was periodically swirled to ensure uniform dissolution of the Sn foil. The molten state was maintained for 20 min to ensure completion of reaction and was then cooled to room temperature. The obtained alloy lump was rolled into ≈ 150 μm foils and were punched into circular discs (diameter = 10 mm) for battery

assembly and testing. For consistency, pure Na metal was prepared using the same melting-cooling process but without addition of Sn.

$Na_3V_2(PO_4)_3$ (NVP)/carbon nanotube composite: First, 1.0 mmol V_2O_5, 3.0 mmol $H_2C_2O_4.2H_2O$ and 3.0 mmol $NaH_2PO_4.2H_2O$ were dissolved in 20 ml water with continuous stirring for 1 hour at 70 °C to obtain a blue solution. A separate solution of 22.8 mg carbon nanotubes (CNTs) dispersed into 50 ml isopropanol with ultrasonic was added to the blue solution. Thereafter, the resulting solution was heated to drying at 70°C . After drying, the precursor was grounded in a mortal and then pretreated at 400 °C for 4 hours and later annealed at 750 °C for 8 hours (5°C /min) under Ar to obtain the final product.

NVP self-supporting cathodes were fabricated by mixing NVP/C, super-P carbon black and PTFE with a weight ratio of 7:2:1. The thin membranes were dried at 70°C overnight under vacuum and were punched into 1.1 cm^2 discs. Typical mass loading was ~ 30 mg cm^{-2}.

Material characterization: X-ray diffraction analysis was carried out on a Rigaku MiniFlex X-ray diffractometer operating at 30 kV and 15 mA using Cu Kα radiation (λ=0.15405 nm). SEM images were collected using a field-emission Hitachi S-4700-II SEM; and EDX spectra were collected using an Bruker Analytical EDS detector. The electrodes for SEM/EDX were washed repeatedly inside a glovebox prior to analysis.

Electrochemical measurements: Electrochemical tests were performed using the type 2025-coin cells. These coin cells were assembled in the glove box using Celgard separator and 1.0 M $NaPF_6$ in diglyme electrolyte. Battery cycling behavior was studied using Neware CT-4008 battery analyzers. Electrochemical impedance data were acquired at room temperature with a frequency range of 0.1 Hz to 100 kHz. Cyclic voltammograms were obtained with a voltage range of -0.1 ~ 0.1V and a scan rate of 0.1 mVs^{-1} using a CH Instruments potentiostat. Full cells were cycled at a voltage range of 2.0 ~ 3.8 V.

2. Supplemental Figures

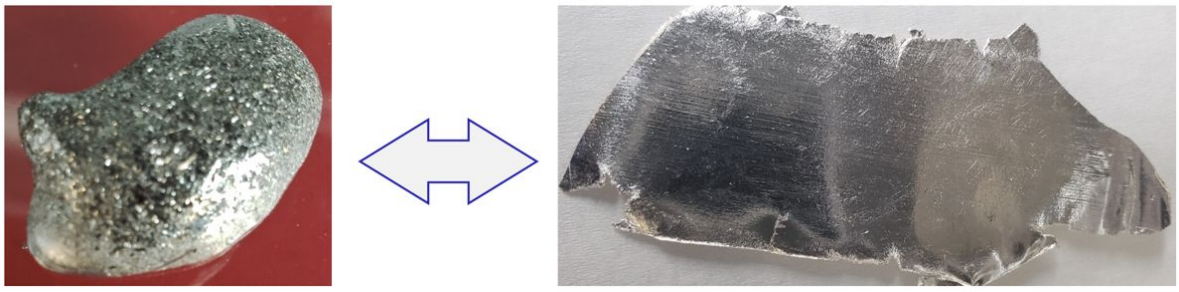

Figure S1: photographs of as-prepared NaSn lump and a piece of NaSn foil.

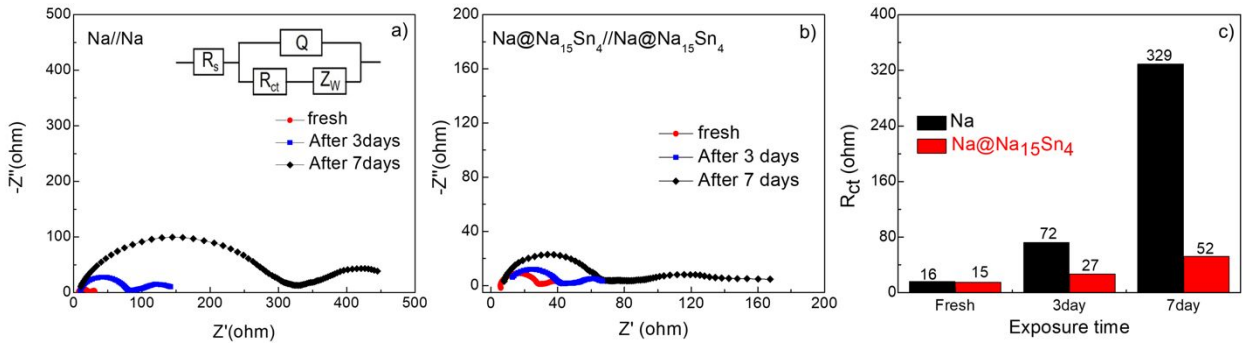

Figure S2: Quantification of surface stability using impedance analysis of symmetric coin cells assembled with a) Na and b) $Na@Na_{15}Sn_4$ electrodes after different days of exposure in glove box; c) comparison of charge transfer resistance extracted using the Nyquist plots and the equivalent circuit model illustrated in a).

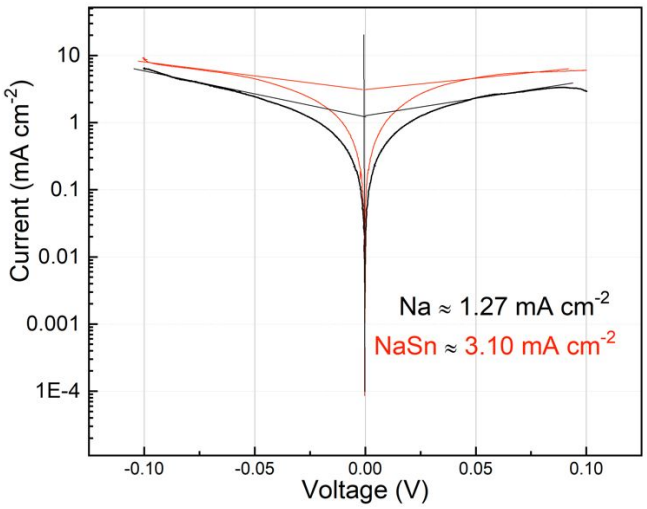

Figure S3: Tafel plot of symmetric coin cells with Na@$Na_{15}Sn_4$ and pristine Na electrodes. The electrolyte was 1.0 M $NaPF_6$ in diglyme.

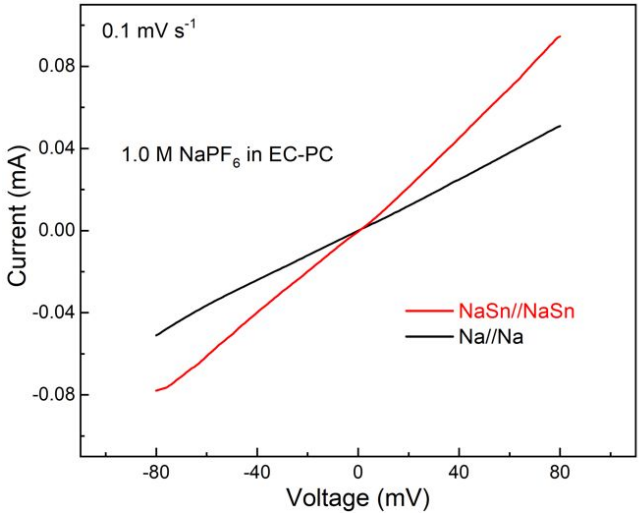

Figure S4: Linear sweep voltammogram of coin cells with symmetric Na@$Na_{15}Sn_4$ and pristine Na electrodes in 1.0 M $NaPF_6$ in ethylene carbonate and propylene carbonate (1:1 vol%).

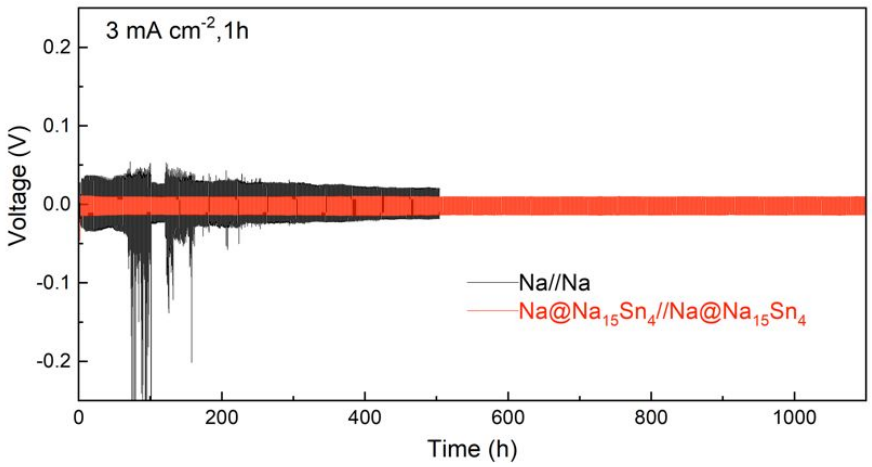

Figure S5: Voltage profiles of symmetric coin cells assembled with $Na@Na_{15}Sn_4$ or pristine Na electrodes at 3.0 mA cm^{-2}.

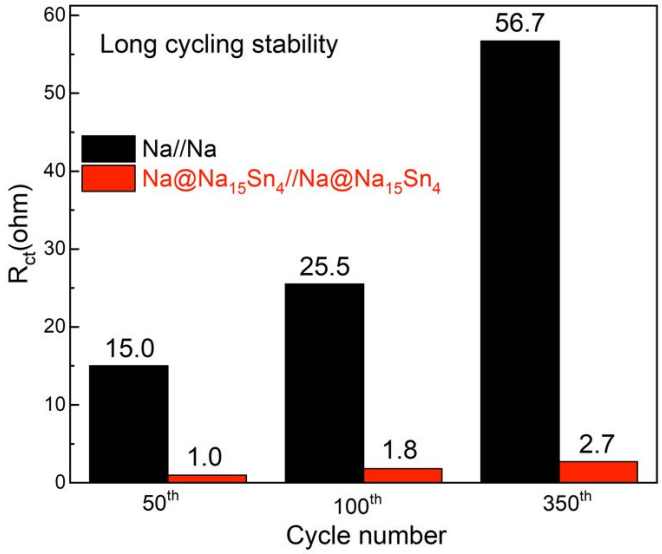

Figure S6: Comparison of changes in charge-transfer resistance (R_{ct}) for symmetric coin cells with either $Na@Na_{15}Sn_4$ or pristine Na electrodes during cycling.

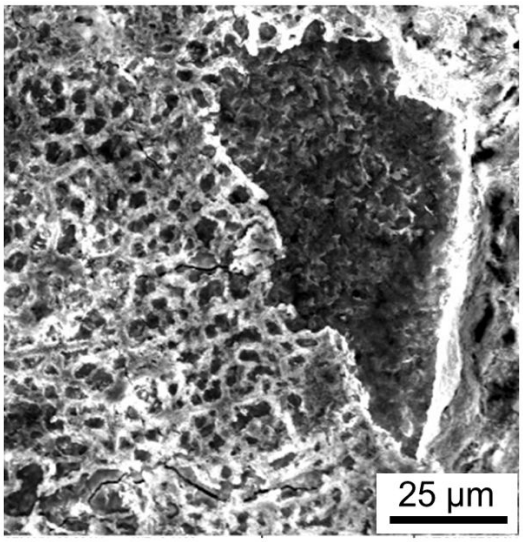

Figure S7: SEM image of pristine Na anode after cycling at 1.0 mA cm^{-2} for 1000 cycles as in a symmetric cell.

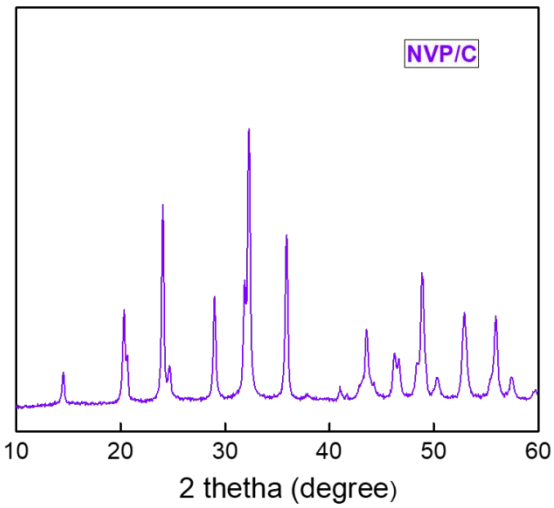

Figure S8: XRD pattern of as-synthesized $Na_3V_2(PO_4)_3$ /C powder.

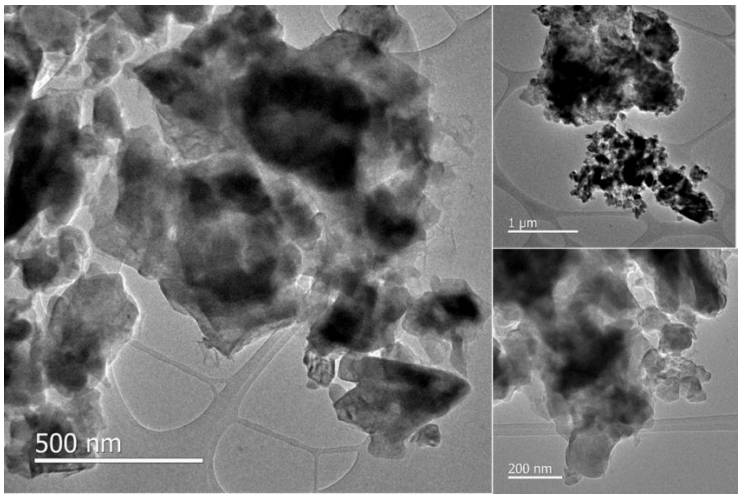

Figure S9: TEM images of as-synthesized $Na_3V_2(PO_4)_3$ /C powders.

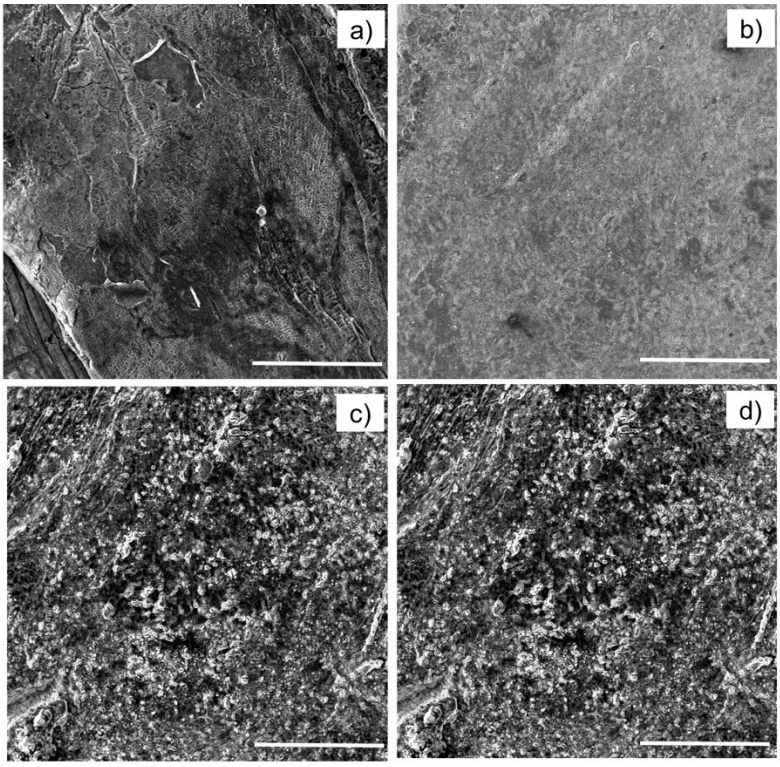

Figure S10: SEM images of a-b) Na@$Na_{15}Sn_4$ and c-d) pure Na electrodes after cycling in full cells, scale bars = 500 µm.

Supplemental Table

Table S1: comparison of the $Na@Na_{15}Sn_4$ composite anode with typical Na anodes reported in the literature

Anode	**cathode**	**electrolyte**	**current density/ mA cm^{-2}**	**capacity / mAh cm^{-2}**	**~ overpotential (cycle)**	**References**
$Na@Na_{15}Sn_4$	$Na@Na_{15}Sn_4$	1.0 M $NaPF_6$-diglyme	5	2.5	≈ 20 (700)	**This work**
$Na@Na_{15}Sn_4$	$Na@Na_{15}Sn_4$	1.0 M $NaPF_6$-diglyme	3	3	≈ 12 (1000)	**This work**
Al_2O_3/Na	Al_2O_3/Na	1.0 M $NaPF_6$-EC/DEC	0.25	0.125	≈ 100 (900)	1
Al_2O_3-PVDF-HFP/Na	Al_2O_3-PVDF-HFP/Na	1.0 M $NaClO_4$-EC/PC	0.5	1	>1000 (127)	2
NaBr/Na	NaBr/Na	1.0 M $NaPF_6$-EC/PC	1	0.5	≈ 150 (250)	3
Al_2O_3/Na	Al_2O_3/Na	1.0 M $NaSO_3$-CF_3-diglyme	3	1	≈ 20 (750)	4
alucone/Na	alucone/Na	1.0 M $NaPF_6$-EC/PC	3	1	≈ 400 (150)	5
graphene/Na	graphene/Na	1.0 M $NaPF_6$-EC/PC	2	3	≈ 450 (100)	6
porous Al/Na	porous Al/Na	1.0M $NaPF_6$-diglyme	0.5	0.5	≈20 (1000)	7
RGO/Na	RGO/Na	1.0M $NaPF_6$-diglyme	1	1	≈ 20 (300)	8
carbonized wood / Na	carbonized wood / Na	1.0M $NaClO_4$-EC/DEC	1	1	>200 (250)	9
carbon fibre/Na	carbon fibre/Na	1M CF_3SO_3Na-diglyme	1	1	≈ 20 (500)	10
Na	Na	5M NaFSI-DME	0.0028	0.0014	>10 (600)	11
Na	Na	$NaAlCl_4.2SO_2$	0.3	0.75	≈ 500 (83)	12

Supplemental References

1. Luo, W.; Lin, C.-F.; Zhao, O.; Noked, M.; Zhang, Y.; Rubloff, G. W.; Hu, L., Ultrathin Surface Coating Enables the Stable Sodium Metal Anode. *Adv. Energy Mater.* **2017,** *7*, 1601526.
2. Kim, Y.-J.; Lee, H.; Noh, H.; Lee, J.; Kim, S.; Ryou, M.-H.; Lee, Y. M.; Kim, H.-T., Enhancing the Cycling Stability of Sodium Metal Electrodes by Building an Inorganic-Organic Composite Protective Layer. *ACS Appl. Mater. Interfaces* **2017,** *9* (7), 6000-6006.
3. Choudhury, S.; Wei, S.; Shin, J. H.; Nath, P.; Agrawal, A.; Archer, L. A.; Ozhabes, Y.; Gunceler, D.; Arias, T. A.; Zachman, M. J.; Kourkoutis, L. F.; Tu, Z., Designing Solid-Liquid interphases for sodium batteries. *Nat. Commun.* **2017,** *8* (1), 898.
4. Zhao, Y.; Goncharova, L. V.; Lushington, A.; Sun, Q.; Yadegari, H.; Wang, B.; Xiao, W.; Li, R.; Sun, X., Superior Stable and Long Life Sodium Metal Anodes Achieved by Atomic Layer Deposition. *Adv. Mater.* **2017,** *29*, 1606663.
5. Zhao, Y.; Goncharova, L. V.; Zhang, Q.; Kaghazchi, P.; Sun, Q.; Lushington, A.; Wang,

B.; Li, R.; Sun, X., Inorganic-Organic Coating via Molecular Layer Deposition Enables Long Life Sodium Metal Anode. *Nano Lett.* **2017,** *17* (9), 5653-5659.
6. Wang, H.; Wang, C.; Matios, E.; Li, W., Critical Role of Ultrathin Graphene Films with Tunable Thickness in Enabling Highly Stable Sodium Metal Anodes. *Nano Lett.* **2017,** *17* (11), 6808-6815.
7. Liu, S.; Tang, S.; Zhang, X.; Wang, A.; Yang, Q.-H.; Luo, J., Porous Al Current Collector for Dendrite-Free Na Metal Anodes. *Nano Lett.* **2017,** *17* (9), 5862-5868.
8. Chi, S.-S.; Qi, X.-G.; Hu, Y.-S.; Fan, L.-Z., 3D Flexible Carbon Felt Host for Highly Stable Sodium Metal Anodes. *Adv. Energy Mater.* **2018,** *8* , 1702764.
9. Zhang, Q.; Lu, Y.; Zhou, M.; Liang, J.; Tao, Z.; Chen, J., Achieving a Stable Na Metal Anode with a 3D Carbon Fibre Scaffold. *Inorg. Chem. Front.* **2018,** *5* (4), 864-869.
10. Wang, A.; Hu, X.; Tang, H.; Zhang, C.; Liu, S.; Yang, Y.-W.; Yang, Q.-H.; Luo, J., Processable and Moldable Sodium-Metal Anodes. *Angew. Chem., Int. Ed.* **2017,** *56* (39), 11921-11926.
11. Lee, J.; Lee, Y.; Lee, J.; Lee, S.-M.; Choi, J.-H.; Kim, H.; Kwon, M.-S.; Kang, K.; Lee, K. T.; Choi, N.-S., Ultraconcentrated Sodium Bis(fluorosulfonyl)imide-Based Electrolytes for High-Performance Sodium Metal Batteries. *ACS Appl. Mater. Interfaces* **2017,** *9* (4), 3723-3732.
12. Song, J.; Jeong, G.; Lee, A.-J.; Park, J. H.; Kim, H.; Kim, Y.-J., Dendrite-Free Polygonal Sodium Deposition with Excellent Interfacial Stability in a $NaAlCl_4$-$2SO_2$ Inorganic Electrolyte. *ACS Appl. Mater. Interfaces* **2015,** *7* (49), 27206-27214.